

Cysteine Scanning Mutagenesis (Residues Glu⁵²–Gly⁹⁶) of the Human P2X1 Receptor for ATP

MAPPING AGONIST BINDING AND CHANNEL GATING^{*†‡}

Received for publication, May 12, 2011, and in revised form, June 16, 2011. Published, JBC Papers in Press, June 20, 2011, DOI 10.1074/jbc.M111.260364

Rebecca C. Allsopp^{‡1}, Sam El Ajouz^{‡1}, Ralf Schmid[§], and Richard J. Evans^{‡2}

From the [‡]Department of Cell Physiology and Pharmacology and [§]Department of Biochemistry, University of Leicester, Leicester LE1 9HN, United Kingdom

P2X receptors are ATP-gated cation channels. The x-ray structure of a P2X4 receptor provided a major advance in understanding the molecular basis of receptor properties. However, how agonists are coordinated, the extent of the binding site, and the contribution of the vestibules in the extracellular domain to ionic permeation have not been addressed. We have used cysteine-scanning mutagenesis to determine the contribution of residues Glu⁵²–Gly⁹⁶ to human P2X1 receptor properties. ATP potency was reduced for the mutants K68C, K70C, and F92C. The efficacy of the partial agonist BzATP was also reduced for several mutants forming the back of the proposed agonist binding site. Molecular docking *in silico* of both ATP and BzATP provided models of the agonist binding site consistent with these data. Individual cysteine mutants had no effect or slightly increased antagonism by suramin or pyridoxal-phosphate-6-azophenyl-2',4'-disulfonate. Mutants at the entrance to and lining the upper vestibule were unaffected by cysteine-reactive methanethiosulfonate (MTS) reagents, suggesting that it does not contribute to ionic permeation. Mutants that were sensitive to modification by MTS reagents were predominantly found either around the proposed ATP binding pocket or on the strands connecting the binding pocket to the transmembrane region and lining the central vestibule. In particular, ATP sensitivity and currents were increased by a positively charged MTS reagent at the G60C mutant at the interface between the central and extracellular vestibule. This suggests that dilation of the base of the central vestibule contributes to gating of the receptor.

P2X receptors are ATP-gated cation channels made from the homo- or heterotrimeric assembly of P2X1 to -7 receptor subunits (1). Their activation mediates a variety of physiological processes, including the neuronal control of smooth muscle contraction, synaptic transmission, taste, and pain sensation, making them novel therapeutic drug targets (2–5). A mutagenesis-based approach has been used to develop an understanding of the molecular basis of agonist action at P2X receptors

because they lack homology with other ATP-binding proteins. A model of the core site of ATP action was proposed with the conserved positive residues Lys⁶⁸, Lys⁷⁰, and Lys³⁰⁹ binding the phosphates, Asn²⁹⁰, Phe²⁹¹, and Arg²⁹² associated with the adenine ring, and a regulatory role of a Phe¹⁸⁵-Thr¹⁸⁶ doublet through polar interactions (6). The publication of a high resolution structure for the zebrafish P2X4 receptor in an agonist free state (7) has been a major advance. The residues predicted to be involved in ATP binding form a cluster between two adjacent subunits (7); however, docking simulations of agonist binding have not been described. The structure also confirms that the second transmembrane segment lines the channel pore. In addition, three vestibules (upper, central, and extracellular) within the extracellular region have been identified (7), and one or a combination of these seems likely to provide a pathway for ions to enter the channel pore.

In this study, we have used cysteine-scanning mutagenesis to investigate the contribution of residues Glu⁵²–Gly⁹⁶ to human P2X1 receptor function (Fig. 2A). This run of residues incorporates five regions of potential importance to receptor function: (i) residues Glu⁵²–Val⁶⁷ link the proposed ATP binding site to the first transmembrane (TM1) segment and therefore could contribute to gating of the channel; (ii) Lys⁶⁸–Lys⁷⁰ has been suggested to have a role in ATP potency; (iii) Leu⁷²–Trp⁸⁵ may contribute to antagonist binding because Lys⁷⁸ plays a role in suramin sensitivity at P2X4 receptors (8); (iv) based on the crystal structure of the P2X4 receptor, the region Asp⁸⁶–Gly⁹⁶ may form the inner face of the predicted ATP binding pocket; and (v) several of the residues are predicted to line the vestibules that pass through the center of the extracellular portion of the receptor. The characterization of cysteine mutants of this region provides a systematic unbiased study of the contribution of these residues to receptor function. We characterized the effects of cysteine mutation on sensitivity to ATP, the efficacy of partial agonists, inhibition by antagonists (suramin and PPADS), and modification by methanethiosulfonate (MTS)³ reagents. These results and previous cysteine-scanning mutagenesis data (6, 9) have been mapped onto a P2X1 receptor homology model and, with docking simulations, provide for the

* This work was supported by the Wellcome Trust and the British Heart Foundation.

⌘ Author's Choice—Final version full access.

† The on-line version of this article (available at <http://www.jbc.org>) contains supplemental Tables i–iii and Fig. 1.

‡ Both authors contributed equally to this work.

§ To whom correspondence should be addressed. Tel.: 44-116-229-7057; Fax: 44-116-252-5045; E-mail: rje6@le.ac.uk.

³ The abbreviations used are: MTS, methanethiosulfonate; BzATP, 2',3'-O-(4-benzoylbenzoyl)-ATP; Ap5A, P¹,P⁵-diadenosine 5'-pentaphosphate; MTSEA, (2-aminoethyl)methanethiosulfonate hydrobromide; MTSES, sodium (2-sulfonatoethyl)methanethiosulfonate; MTSET, [2-(trimethylammonium) ethyl]methanethiosulfonate bromide; α,β -meATP, α,β -methyl-ene ATP; PPADS, pyridoxal-phosphate-6-azophenyl-2',4'-disulfonate.

Agonist Binding and Gating of P2X1 Receptors

first time a model of agonists docked to the receptor, identify a ring of charge between the central and extracellular vestibule associated with channel gating, and suggest that the upper and central vestibules do not contribute to the ionic permeation pathway.

EXPERIMENTAL PROCEDURES

Site-directed Mutagenesis—Cysteine point mutations for residues Glu⁵²–Gly⁹⁶ were introduced via the QuikChange mutagenesis kit (Stratagene, La Jolla, CA) using the human P2X1 receptor plasmid as the template, as described previously (10). Production of the correct mutations and absence of coding errors in the P2X1 mutant constructs were verified by DNA sequencing (Automated ABI Sequencing Service, University of Leicester).

Expression in *Xenopus laevis* Oocytes—Wild type and mutant constructs were transcribed to produce sense strand cRNA (mMessage mMachine, Ambion, Austin, TX) as described previously (10). Manually defolliculated stage V *X. laevis* oocytes were injected with 50 nl (50 ng) of cRNA using an inject + Matic microinjector (L. A. Gaby, Inject + Matic, Genève, Switzerland) and stored at 17 °C in ND96 buffer (96 mM NaCl, 2 mM KCl, 1.8 mM CaCl₂, 1 mM MgCl₂, 5 mM sodium pyruvate, 5 mM HEPES, pH 7.6). Medium was changed daily prior to recording 3–7 days later.

Electrophysiological Recordings—Two-electrode voltage clamp recordings (at a holding potential of –60 mV) were performed on cRNA-injected oocytes using a GeneClamp 500B amplifier with a Digidata 1322 analog-to-digital converter and pClamp 8.2 acquisition software (Axon Instruments, Molecular Devices, Foster City, CA), as described previously (10). Native oocyte calcium activated chloride currents in response to P2X receptor stimulation were reduced by replacing 1.8 mM CaCl₂ with 1.8 mM BaCl₂ in the ND96 bath solution. ATP (magnesium salt) was applied via a U-tube perfusion system, as were BzATP and Ap5A (all from Sigma). Agonists were applied usually for 3 s at 5-min intervals. Using this regime, reproducible agonist-evoked responses were recorded. Individual normalized concentration-response curves were fitted with the Hill equation, $Y = X^H / (X^H + EC_{50}^H)$, where Y is response, X is agonist concentration, H is the Hill coefficient, and EC_{50} is the concentration of agonist evoking 50% of the maximum response. pEC_{50} is the $-\log_{10}$ of the EC_{50} value. For the calculation of EC_{50} values, individual concentration response curves were generated for each experiment, and statistical analysis was carried out on the pEC_{50} data generated. In the figures, concentration response curves are fitted to the mean normalized data.

³²P-Labeled 2-Azido-ATP Binding Assay—To assess any effects of mutation on agonist binding, we used a ³²P-labeled 2-azido-ATP binding assay for WT, K68C, K70C, and F92C mutants, as described previously (6).

Effects of Methanethiosulfonate Compounds—To study the effect of MTS compounds on wild type and cysteine mutants, ATP (~ EC_{50} concentration) was applied, and MTSEA, MTSES, or MTSET (Toronto Research Chemicals, Toronto, Canada) was bath-perfused (for at least 5 min; the recovery time required between application to see reproducible responses) prior to co-application with ATP via the U-tube. MTS reagents

(1 mM) were made in ND96 solution immediately prior to use. The effect of MTS reagents on the concentration responses to ATP was investigated by application of ATP in the presence of MTS reagents or following a 3-h incubation of oocytes in MTS reagents and then subsequent ATP application via the U-tube with ND96 bathing solution (no MTS reagents present). The same results were found with either method.

Characterizing the Effects of Antagonists—Suramin or PPADS was perfused in the bath as well as co-applied with ATP from the U-tube. To investigate the effects of cysteine mutation on antagonist sensitivity, a concentration of antagonist that reduced the EC_{90} concentration of ATP response by half at WT P2X1 receptors (either 3 μ M suramin or 3 μ M PPADS) was applied to the P2X1 receptor mutants. Schild analysis was used to estimate the pK_B of suramin.

Analysis—All data are shown as means \pm S.E. Significant differences between WT and mutants were calculated by one-way analysis of variance followed by Dunnett's test for comparisons of individual mutants against control using GraphPad Prism 5 (GraphPad Software Inc., San Diego, CA). The significance of any changes in ATP potency by MTS compounds was determined with the appropriate Student's t test. n corresponds to the number of oocytes tested for electrophysiological data, and for biochemical studies, experiments were repeated at least three times.

Molecular Modeling—The trimeric assembly of the human P2X1 receptor (residues 33–352) was modeled in Modeler version 9.7 (11) based on the zebrafish P2X4 structure (Protein Data Bank code 3I5D) as template. Target and template share 44% sequence identity and 67% sequence similarity based on a BLAST alignment. Of the models generated, the best model was selected based on Modeler's scoring function and external validation via Whatcheck (12) and PROSA (13). This model then served as the starting structure for ligand docking with ATP and BzATP. In preparation for ligand docking, atomic coordinates for ATP were extracted from the Protein Data Bank (entry 1HCK). Hydrogens were added in Hyperchem 8.0 (Hypercube Inc., Gainesville, FL) using the MM+ force field to generate two alternative protonation states, ATP3- and ATP2-, followed by steepest descent energy minimization until convergence. In a similar way, BzATP was built and optimized based on the energy-minimized ATP structure. Both ATP and BzATP were docked into the P2X1 homology model using the GOLD package (14). The approximate location of the ATP binding site was set based on previous work (15) and defined as all residues within a 20-Å sphere centered at the Phe²⁹¹ backbone nitrogen. The side chains of residues Lys⁶⁸, Lys⁷⁰, Arg²⁹², and Lys³⁰⁹ were treated as flexible using the "flexible side chain-library" option in GOLD to better accommodate the triphosphate moiety of ATP. The resulting docking poses were ranked by their GOLDScores and inspected manually. All figures illustrating molecular modeling results were prepared in PyMOL (version 1.2r3; Schrödinger, LLC), and internal cavities were visualized using the Hollow tool (16).

RESULTS

Effects of Cysteine Point Mutations on ATP Sensitivity—The region Glu⁵²–Gly⁹⁶ spans from the first transmembrane

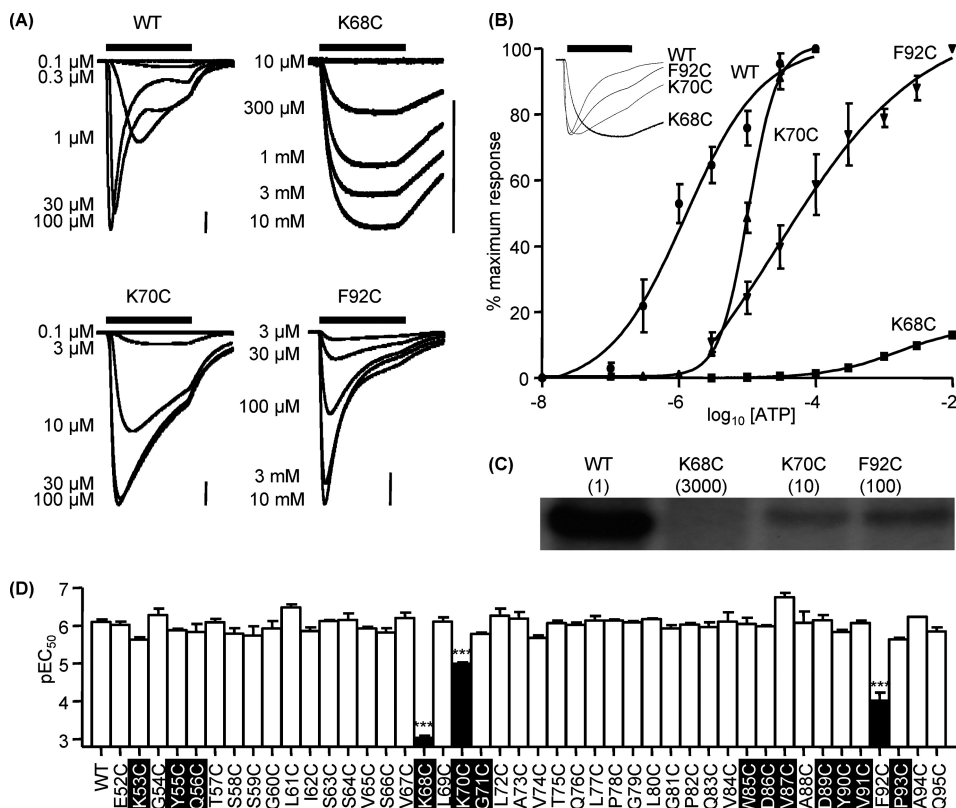


FIGURE 1. Effect of point cysteine mutations on ATP potency. Agonist action was tested on P2X1 WT and P2X1 receptor mutants expressed in oocytes by two-electrode voltage clamp (holding potential, -60 mV). *A*, concentration responses to ATP for oocytes expressing WT, K68C, K70C, and F92C mutant P2X1 receptors. ATP was applied for 3 s (indicated by the *black bar*; scale bar, 1 μA for all). *B*, summary of concentration response data for WT and mutants K68C, K70C, and F92C, which showed a significant decrease in ATP potency ($n = 3-4$). Error bars, S.E. The *inset* represents the slower response times of K68C, K70C, and F92C compared with WT in response to a maximum concentration of ATP. *C*, autoradiograph depicting radiolabeled $[^{32}\text{P}]2$ -azido-ATP cross-linked to WT and mutant receptors (mean EC_{50} for ATP (in μM) is shown in *parentheses*). *D*, summary showing pEC_{50} values of all mutants compared with WT (*left*). Values are shown as means \pm S.E. Significant differences from the wild type are indicated (***) $p < 0.001$. Conserved residues are *highlighted in black*.

domain up through the inner vestibule of the channel to the proposed ATP binding site and then loops back to the rear of the agonist binding pocket (Fig. 2*A*). The contribution of individual residues in this region to receptor properties was determined by cysteine-scanning mutagenesis. ATP evoked concentration-dependent P2X1 receptor-mediated currents from WT receptors with an EC_{50} of ~ 1 μM (Fig. 1, *A* and *B*) and responses to a maximal concentration of ATP desensitized during the continued presence of agonist (time to decay from the peak to 50% was 949 ± 162 ms) as reported previously (10). For the majority of mutants tested in the run Glu⁵²–Gln⁹⁵ (42 of 45), cysteine substitution had no effect on ATP sensitivity or peak current amplitude (Fig. 1*D* and [supplemental Table i](#)) (we have previously reported the G96C results in a modest 4-fold decrease in ATP sensitivity (17)). Interestingly, mutation of the residues equivalent to Gln⁵⁶ and Asp⁸⁹ in the P2X2 receptor (Q56C and E85A (18, 19)) were non-functional, suggesting that there are subtype differences in the ability to tolerate mutation. ATP sensitivity was reduced by >3000 -fold at the K68C mutant (saturating concentration response curves could not be generated, and the EC_{50} was estimated to be >3 mM). ATP currents at the K68C mutant evoked by the highest concentration of agonist tested (10 mM) also showed little decline during a 3-s application ($0.75 \pm 0.49\%$ decline, $n = 8$), and the time to 50% decay was ~ 35 -fold slower (774 ± 114 and $28,815 \pm 2037$ ms for WT and K68C respectively, $n = 6$) than for WT recep-

tors. Peak currents to a maximal concentration of ATP were also reduced by $\sim 90\%$ (992 ± 88 and 8503 ± 577 nA for K68C and WT, respectively, $p < 0.001$). However, Western blot analysis showed that the level of both total and surface expression of the K68C mutant receptors was equivalent to WT (data not shown), indicating that reduced current amplitude does not result from a decrease in receptor expression. K70C showed a modest 10-fold decrease in ATP potency ($\text{EC}_{50} \sim 10$ μM , $p < 0.001$), with no change in peak amplitude. ATP potency was also reduced by almost 100-fold at the F92C mutant receptor ($\text{EC}_{50} \sim 100$ μM , $p < 0.001$), with no change in peak amplitude.

The decrease in ATP potency for the mutants K68C, K70C, and F92C could result from an effect on agonist binding and/or channel gating. Because WT and K68C, K70C, and F92C mutants are expressed at the same level on the cell surface (data not shown), a 2-azido-ATP binding assay was used to gain insight into the mechanisms underlying the changes in potency (6, 9). Radiolabeled 2-azido ATP incorporation following photoactivation was reduced by 84.0 ± 3.7 , 55.2 ± 4.2 , and $46.2 \pm 4.2\%$ compared with WT for K68C, K70C, and F92C, respectively ($p < 0.001$ for K68C, and $p < 0.01$ for K70C and F92C; Fig. 1*C*). The reductions in 2-azido-ATP labeling at K68C and K70C are consistent with the proposed contribution of these residues to binding the negative charge of the phosphate of ATP. For F92C, 2-azido-ATP binding was reduced to a similar extent as that for K70C; however, ATP sensitivity was 10-fold

Agonist Binding and Gating of P2X1 Receptors

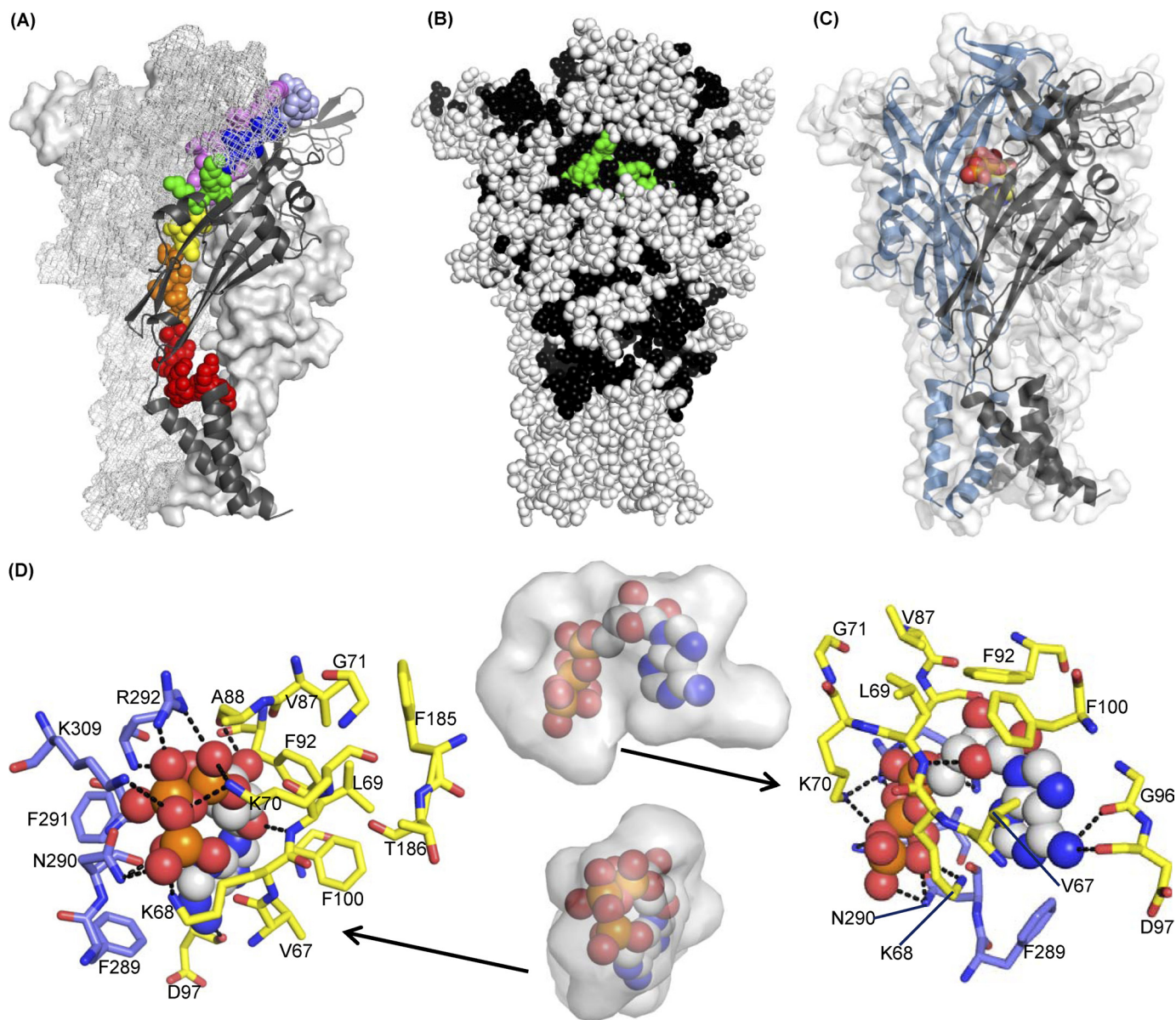


FIGURE 2. Homology model and ATP docking for the P2X1 trimer. Images were generated in PyMOL. *A*, overview of the P2X1 homology model, highlighting residues 52–96. Residues studied by cysteine-scanning mutagenesis are displayed as spheres in rainbow colors (red, Glu⁵²–Ser⁵⁹; orange, Gly⁶⁰–Ser⁶⁴; yellow, Val⁶⁵–Val⁶⁷; green, Lys⁶⁸–Lys⁷⁰; blue, Gly⁷¹–Thr⁷⁵; indigo, Gln⁷⁶–Leu⁸⁰; violet, Gly⁸¹–Gly⁹⁶) for the P2X1 subunit in the front of the picture. The overall structure of this subunit is shown in a black schematic representation, whereas the two P2X1 subunits in the background are shown in a surface and grid representation, respectively. *B*, mapping of mutation data onto the P2X1 homology model. All residues are shown as spheres. Residues colored black have been tested for their contributions to ATP sensitivity. Of these, residues that make substantial contributions to ATP sensitivity are highlighted in green (Lys⁶⁸, Lys⁷⁰, Phe⁹², Thr¹⁸⁶, Asn²⁹⁰, Phe²⁹¹, and Arg²⁹²). Residues not tested are shown in white. To give a more complete picture, previously published data for residues Glu¹⁸¹–Val²⁰⁰ and Ser²⁸⁶–Ile³²⁹ have been included in addition to residues Glu⁵²–Gly⁹⁶. *C*, overview of the P2X1 model showing the ATP binding site and the predicted ATP binding pose. The three subunits of P2X1 (residues 33–352) are shown in schematic representations in blue, black, and gray, respectively. One docked ATP molecule located at the interface between two subunits is displayed as spheres in CPK colors. The overall shape of the P2X1 model is indicated by the semitransparent surface for all three subunits. *D*, zoom into the ATP-binding site from the front (left) and rear (right). The best scoring docked pose of ATP is shown as spheres. Residues within 3 Å of ATP are shown as sticks, the blue and yellow colors indicating different subunits of the P2X1 trimer. Predicted hydrogen bonds are plotted as dotted lines in black. The middle panel illustrates the available space in the ATP binding cavity as determined by a hollow for both views. The volume of the cavity is shown as a transparent surface representation with the docked ATP in spheres.

further reduced for the F92C mutant compared with K70C. This suggests that in addition to a role on agonist binding, Phe⁹² may also contribute to the subsequent gating of the P2X1 receptor, and this combined effect accounts for the reduction in ATP potency.

Homology Modeling, Mutant Mapping, and Agonist Docking—The results of the present study highlight a role of residues Lys⁶⁸, Lys⁷⁰, and Phe⁹² in ATP action at the P2X1

receptor. A homology model for the human P2X1 receptor was generated to visualize the effects of site-directed mutagenesis in a structural context (Fig. 2, A and B). Based on the knowledge of key residues involved in ATP binding, ligand docking was used to model the ATP binding site in detail (Fig. 2, C and D). The output of the P2X1-ATP ligand docking experiment is a ranked list of potential poses of ATP binding to the P2X receptor. Strikingly, the solutions with the highest GOLD fitness scores in the

docking experiment have some key features in common; the positively charged residues Lys⁶⁸, Lys⁷⁰, Arg²⁹², and Lys³⁰⁹ and the NH₂-amide of Asn²⁹⁰ coordinate the partially negatively charged oxygens of the phosphate moiety. The adenine ring is centered in a hydrophobic pocket formed by Val⁶⁷, Phe¹⁰⁰, Phe²⁸⁹, and Phe²⁹¹. For the amino group of the ATP-adenine, the best ranked solution predicts two hydrogen bonds to the backbone carbonyls of Gly⁹⁶ (reduced ATP potency for cysteine mutant (17) and reduced partial agonist effects) and Asp⁹⁷. The ribose is predicted to be close to Phe⁹² (consistent with the decrease in ATP potency at F92C); the best ranked solution suggests that Leu⁶⁹ donates an hydrogen bond to the ring oxygen of the ATP-ribose, whereas the backbone carbonyl of Ala⁸⁸ interacts with the 3'-hydroxy group of the ATP-ribose. Mutations at the conserved doublet Phe¹⁸⁵-Thr¹⁸⁶ (P2X1 receptor numbering) can affect ATP potency (6, 20). However, these conserved residues (185,186 P2X1 receptor numbering) are at least ~5–7 Å from the closest atom of the docked ATP in the model and in this conformation are unlikely to interact directly with the agonist. It thus seems likely that these residues may be involved in conformational changes associated with agonist binding and/or gating of the channel. These could arise from interactions with other parts of the receptor; one possibility could be an interaction with the cysteine-rich head region. At P2X2 and P2X3 receptors, mutation of the conserved glycine equivalent to residue 71 (P2X1 numbering) reduced ATP potency (21, 22). The lack of effect of the G71C mutation in the present study indicates differences between the subunits that may contribute to their variations in pharmacology. Overall, the docking based predictions are consistent with our mutagenesis studies on the P2X1 receptor and provide a structure/docking-based working model of the ATP binding site.

Partial Agonists Identify Additional Residues Involved in Agonist Action and Allow Testing of the Model of the Proposed ATP Binding Site—The efficacy of partial agonists provides a sensitive measure of changes in agonist action. For example, at WT receptors, BzATP is equipotent with ATP but is a partial agonist with an efficacy of ~0.45–0.5 (20). At the majority of mutants (32 of 45), there was no change in efficacy for BzATP compared with WT receptors (supplemental Table i). For the mutants K68C, K70C, and F92C that decreased ATP potency, the partial agonist BzATP (100 μM) was essentially ineffective (Fig. 3, A and B). Although 100 μM BzATP is not a maximal concentration at these mutants, from studies on the WT receptor, where BzATP is equipotent, one would predict that a response of ~40% of that of ATP should still be recorded if there was no change in efficacy. There were 10 mutants that showed no change in ATP sensitivity where BzATP activity was either increased (>80% maximum response to ATP for L72C and A73C), decreased by about half (I62C, G81C, W85C, Q95C, and G96C), or almost abolished (T75C, Y90C, and P93C) (Fig. 3, A and B, and supplemental Table i). For mutants where the response was reduced or abolished, there was no difference in efficacy between 10 and 100 μM BzATP, indicating that there had not been a decrease in potency. These results show that the partial agonist BzATP can be useful in characterizing subtle changes in agonist action at P2X1 receptors. Mapping these mutants onto the homology model of the P2X1 receptor shows

that they are predominantly clustered around the predicted ATP binding site (Fig. 3, C–E).

The agonist actions of BzATP are also of particular interest because they allow further testing of the ATP binding site model. The substitutions of the benzoyl groups on the ribose ring are quite large and would need to be accommodated in the agonist binding pocket. Molecular docking simulations for BzATP are less conclusive than the ATP docking. The most plausible solutions find the phosphate moiety of BzATP in a similar orientation as in the docked ATP, forming polar interactions with the side chains of Lys⁷⁰, Asn²⁹⁰, Arg²⁹², Lys³⁰⁹, and (less pronounced) Lys⁶⁸. In these solutions, the adenine and ribose rings of BzATP are slightly rotated compared with ATP so that the 3'-O-4-benzoyl-benzoyl substituent protrudes along Asp⁸⁹, Tyr⁹⁰, Phe⁹², and Pro⁹³ (see Fig. 3E). Similar orientations and docking scores were found for the 2'-O-isomere, so the ligand docking results do not predict any preference for one of the two BzATP isomers. These results indicate that BzATP can be accommodated within the predicted ligand binding pocket and have an orientation similar to that of ATP.

For those mutants with a change in efficacy to BzATP, we also determined whether there was an equivalent change for the partial agonists Ap5A and α,β-meATP (applied at 100 μM, these agonists have potency similar to that of ATP (20, 23). At WT receptors, the efficacy of Ap5A and α,β-meATP was 0.40 ± 0.09 and 0.56 ± 0.09, respectively (n = 5). The pattern of changes in efficacy for Ap5A was the same as for BzATP for the majority of mutants (increases for L72C and A73C and decreases in efficacy K68C, K70C, T75C, G81C, Y90C, F92C, P93C, Q95C, and G96C) (Fig. 3F). However, there was no change in efficacy for Ap5A compared with WT for mutants I62C and W85C. For α,β-meATP, L72C and A73C mutants showed increased efficacy, and only K68C, K70C, and F92C showed a significant decrease in efficacy compared with WT (Fig. 3G).

These results show that partial agonists can reveal subtle changes in properties of the P2X receptor not seen for ATP and that they can be used to classify mutants into four groups: (i) those with a decrease in ATP potency and partial agonists (K68C, K70C, and F92C), (ii) those with an increase in efficacy to all three partial agonists with no change in ATP sensitivity (L72C and A73C), (iii) agonist-dependent efficacy changes (T75C, G81C, Y90C, F92C, P93C, and Q95C; reductions in BzATP and Ap5A efficacy but no effect on α,β-meATP), and (iv) those least sensitive to partial agonists (I62C and W85C; efficacy reduction only for BzATP).

Antagonist Action at P2X1 Receptor Mutants—Suramin and PPADS are antagonists at P2X receptors (24, 25), and residues around the proposed ATP binding groove have been shown to be involved in antagonist sensitivity (7). In the region Glu⁵²–Gly⁹⁶, suramin sensitivity has been associated with Lys⁷⁸ in the P2X4 receptor (8), and a recent study on P2X2 receptors has modeled suramin derivative docking within the predicted ATP binding pocket with interactions with residues equivalent to Lys⁷⁰ and Gly⁷¹ (22).

Suramin produced a parallel rightward shift in the concentration-response curve to ATP at WT P2X1 receptors indicative of a competitive antagonist (supplemental Fig. 1). At WT

Agonist Binding and Gating of P2X1 Receptors

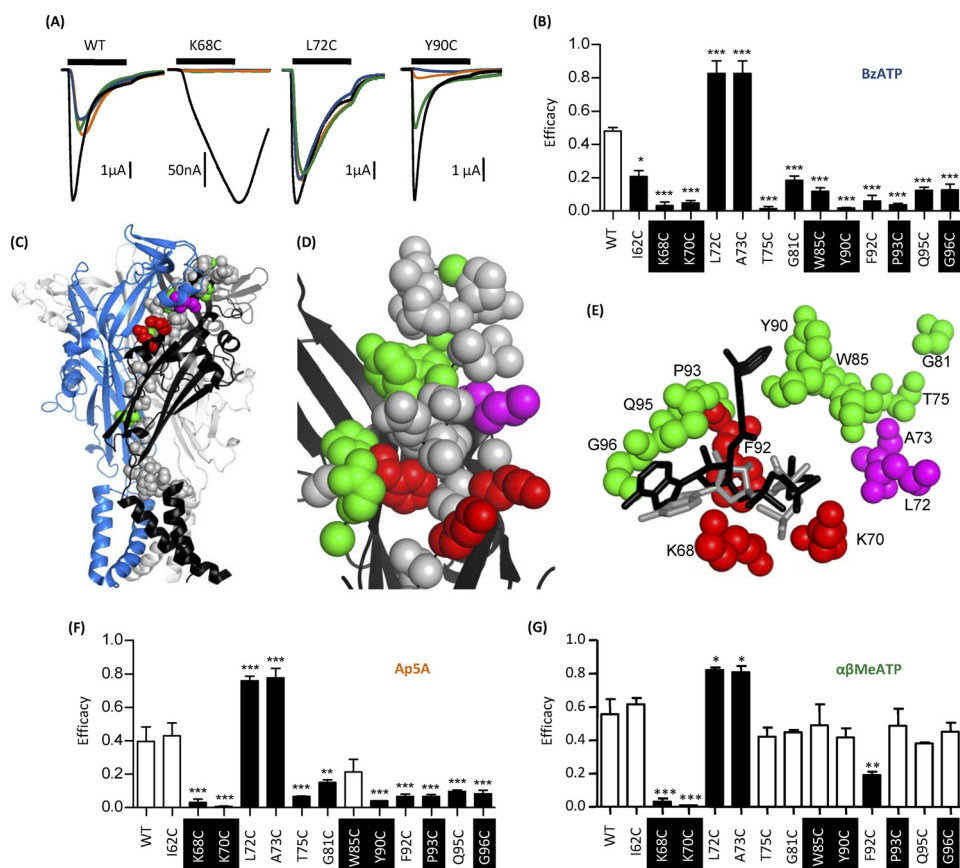


FIGURE 3. Effect of cysteine point mutations on partial agonist efficacy. Partial agonist action was tested on WT and P2X1 receptor mutants expressed in oocytes by two-electrode voltage clamp (holding potential, -60 mV). *A*, representative recordings of currents evoked by partial agonists ($100 \mu\text{M}$) compared with control ATP ($100 \mu\text{M}$) (black) for WT and mutants K68C, L72C, and Y90C. K68C and Y90C both show a decrease in efficacy of BzATP (blue) compared with the variable sensitivity of AP5A (amber) and α,β -MeATP (green), with L72C having an increased efficacy of all of the partial agonists. *B*, summary of all mutants demonstrating significant changes in efficacy of BzATP. *C*, schematic representation of the P2X1 receptor homology model; mutants that modified BzATP efficacy are shown as spheres. Red, decrease in ATP potency and reduced BzATP efficacy; green, no effect on ATP potency and reduced efficacy; magenta, no effect on ATP potency and increased efficacy. *D*, higher magnification of the region around the proposed ATP binding pocket showing mutants that change BzATP efficacy (same coloring as in *C*). *E*, molecular docking of BzATP to the P2X1 receptor shows that BzATP can fit within the proposed ATP binding pocket. Docking is shown for both ATP (in gray) and BzATP (in black), and residues that modified BzATP efficacy are shown (same coloring as in *C* and *D*). *F* and *G*, the effect of AP5A and α,β -MeATP on the corresponding mutants. Significant changes in efficacy are shown as black bars. *, $p < 0.05$; **, $p < 0.01$; ***, $p < 0.001$. Conserved residues are highlighted in black. Error bars, S.E.

P2X1 receptors, an EC_{50} concentration of ATP ($10 \mu\text{M}$) was reduced by 50% ($52 \pm 2\%$) by $3 \mu\text{M}$ suramin. Testing of the effects of this concentration of suramin on an EC_{50} concentration of ATP at the cysteine mutants provided a sensitive assay to detect any changes in antagonist action. There was no change in suramin sensitivity for the majority of mutants (37 of 45). However, there was an increase in sensitivity at the mutants Y55C, K68C, K70C, G71C, T75C, Y90C, P93C, and Q85C (Fig. 4, A–C). Interestingly, for the majority of these mutants (six of eight), this increase in suramin antagonism was associated with a decrease in sensitivity to the partial agonist BzATP (supplemental Table i). A Schild analysis of the actions of suramin was determined for the mutant with the greatest increase in suramin action (Y90C). At the Y90C mutant, suramin had a pA_2 of 7.2 (slope 1.15), an ~ 3 -fold higher affinity than for the WT (pA_2 of 6.7, slope 0.93) (Fig. 4B).

PPADS acted as a noncompetitive antagonist and decreased the amplitude of ATP-evoked currents at WT P2X1 receptors with no change in the time course or the EC_{50} value (Fig. 4 and supplemental Fig. 1). The response to an EC_{50} concentration of ATP at P2X1 WT receptors was reduced by $\sim 50\%$ ($44 \pm 7\%$) by

$1 \mu\text{M}$ PPADS, and this paradigm was used to test for any changes in PPADS sensitivity for the cysteine mutants. There was no change in sensitivity to PPADS for any of the cysteine mutants with the exception of I62C, where $1 \mu\text{M}$ PPADS was more effective and reduced the response to an EC_{50} concentration of ATP by $94 \pm 3\%$ (Fig. 4, A and C). These results suggest that individual residues in the region Glu⁵²–Gly⁹⁶, including those within the predicted ATP binding pocket, do not make a major contribution to suramin or PPADS sensitivity at the P2X1 receptor.

Effects of Charged Methanethiosulfonate Reagents on Cysteine Mutants—Thiol-reactive MTS reagents have previously been used to modify accessible cysteine residues and investigate a range of ion channels, including P2X receptors (26, 27). In this study, we tested the effects of negatively charged MTSES and the larger positively charged MTSET on current amplitude and ATP potency at the cysteine mutants. For WT P2X1 receptors, MTSES (1 mM) had no effect on receptor currents in response to an EC_{50} concentration of ATP (Fig. 5), as previously reported (9) and consistent with a lack of free cysteine residues in the native receptor. For the majority of mutants (35 of 45), MTSES

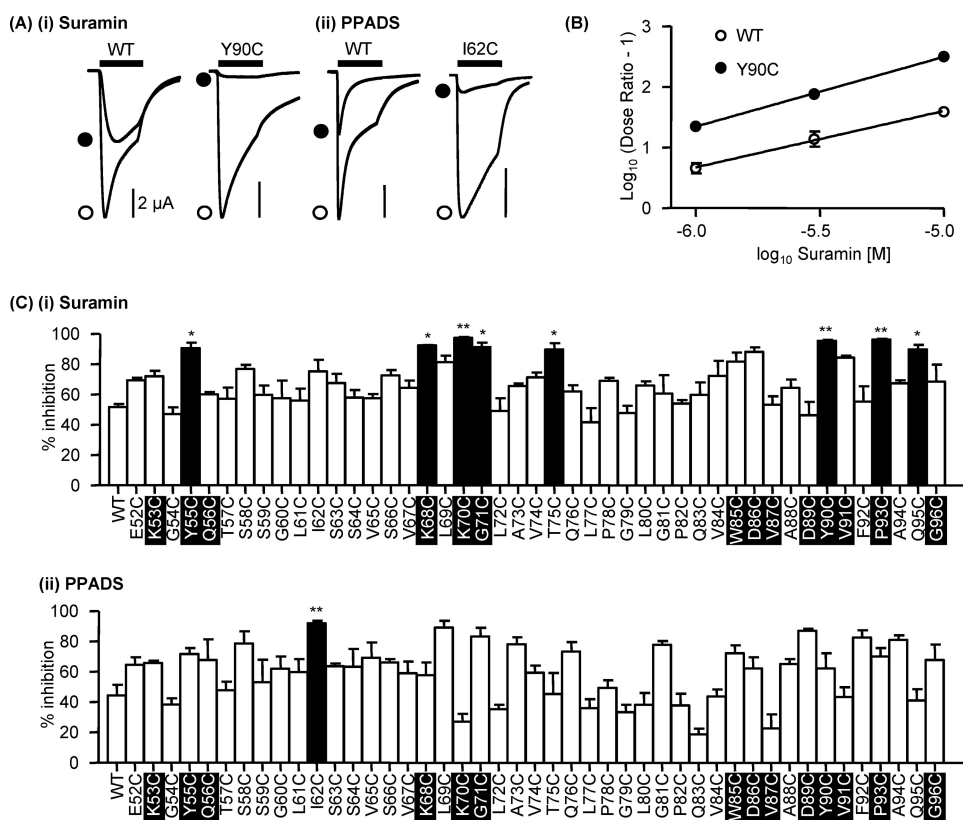


FIGURE 4. Antagonist action at P2X1 receptor mutants E52C to G96C. An EC_{50} concentration of ATP was applied to oocytes expressing P2X1 WT and P2X1 receptor mutants E52C to G96C. Antagonists were applied to the P2X1 receptor using concentrations that inhibited the WT response by $\sim 50\%$, suramin ($3 \mu M$) and PPADS ($1 \mu M$). *A*, representative recordings of Y90C (i), a P2X1 mutant with increased suramin sensitivity, and I62C, a P2X1 mutant with increased PPADS sensitivity (ii). Traces show the response in the presence of ATP only (open circle) and in the presence of ATP and the antagonist (closed circle). ATP was applied for 3 s (black bar), and the antagonists were bath-perfused 5 min before recording. *B*, Schild plot analysis of suramin antagonism at the WT P2X1 receptor and the mutant Y90C. *C*, percentage inhibition of EC_{50} concentration of ATP in the presence of the antagonists suramin ($3 \mu M$) (i) and PPADS ($1 \mu M$) (ii) on P2X1 receptor mutants E52C to G96C ($n = 3-4$). *, $p < 0.05$; **, $p < 0.01$. Error bars, S.E. Conserved residues are highlighted in black.

had no effect. However, responses were significantly inhibited at I62C, S63C, K68C, K70C, L72C, P82C, D86C, V87C, P93C, and G96C mutants (Fig. 5). Mutants that were reduced by MTSES were investigated further to determine whether ATP sensitivity and responses to a maximal concentration of ATP were also affected. For the mutants I62C, S63C, L72C, P82C, and D86C, MTSES reduced the response to a maximal concentration of ATP but had no effect on agonist potency (supplemental Table ii), suggesting an effect on the conformational change associated with channel opening subsequent to agonist binding. In addition to a reduction in the amplitude of currents to a maximal concentration of ATP, MTSES also reduced ATP potency for the K70C mutant by ~ 14 -fold and by $\sim 3-4$ -fold for V87C, P93C, and G96C (Fig. 6 and supplemental Table ii). For K68C, responses even to a maximal concentration of ATP (10 mM) were abolished by MTSES.

We also tested the effects of positively charged MTSET (larger than MTSES). MTSET had a small effect on the response to an EC_{50} concentration of ATP, increasing it by $10 \pm 8\%$ at WT P2X1 receptors, consistent with previous findings (6, 9). For the majority of mutants (40 of 45), there was no significant change in the response to MTSET compared with the wild type (Fig. 5). At mutant S66C, responses were no different from WT with MTSET; this contrasts with studies on the P2X2 receptor, where ATP responses at the equivalent mutant (I67C)

were reduced (18), and mapping this residue onto the homology model showed that it is deeper in the structure at the interface of adjacent subunits and is unlikely to contribute directly to the ligand binding pocket. The effects of MTS reagents at the P2X2 receptor may therefore result from effects on channel conformational changes or interaction with residues that are variant between the P2X1 and P2X2 receptors (there is a two-amino acid insertion of KY in the P2X2 receptor with the loop around residues 282–285 that is close to the residue Ser⁶⁶). The response to ATP was potentiated for mutants G60C and V91C even to a maximal concentration of ATP (by 58 and 25%, respectively; Figs. 5 and 6 and supplemental Table iii). The potency of ATP was also increased ~ 6 -fold following MTSET treatment for the G60C mutant (but not for V91C) (Fig. 6A and supplemental Table iii). For mutants S64C and K70C, MTSET had no effect on ATP potency but reduced the amplitude of responses even to a maximal concentration of ATP by $\sim 55\%$ (Fig. 6 and supplemental Table iii). MTSET abolished responses to the maximal concentration of ATP tested (10 mM) for the K68C mutant (Fig. 6C). This is consistent with previous mutagenesis studies showing that the mutation to replace Lys⁶⁸ with the larger positively charged Arg abolished ATP-evoked responses (10). We previously showed that ATP potency is reduced for the mutants K309C at the P2X1 receptor and K68C and K70C for the P2X4 receptor, and this can be rescued by the

Agonist Binding and Gating of P2X1 Receptors

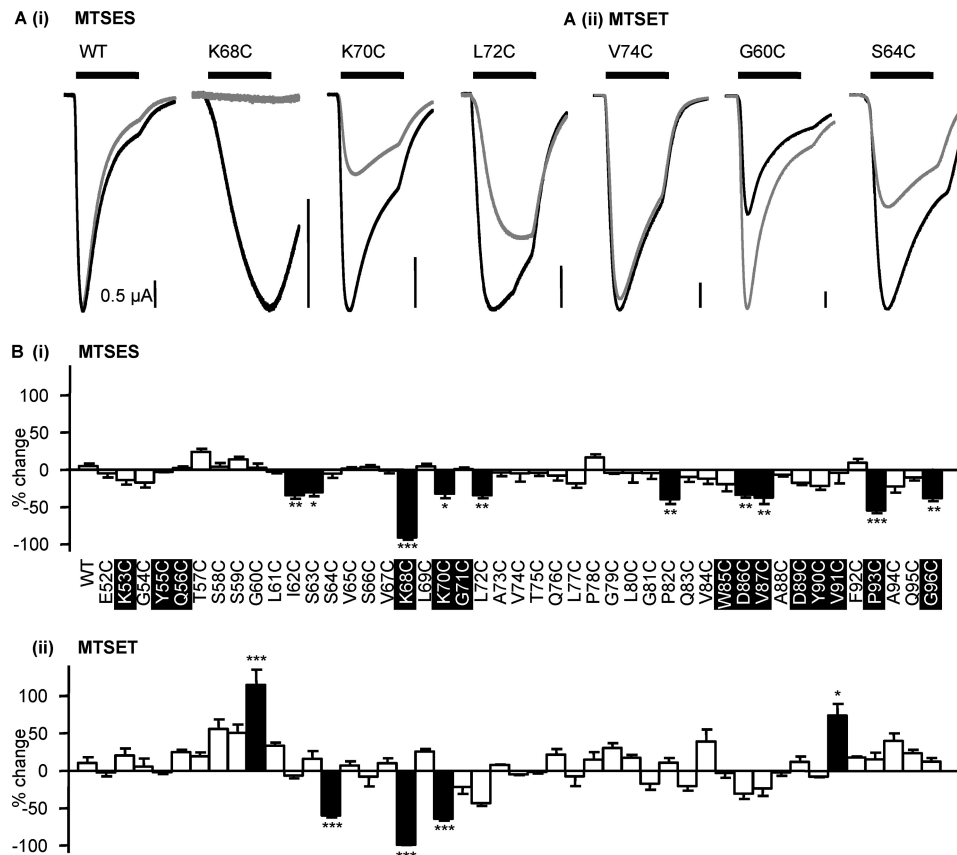


FIGURE 5. **Effect of MTS reagents at P2X1 receptor mutants E52C to G96C.** *A*, effect of MTSES (*i*) and MTSET (*ii*) on an EC_{50} concentration of ATP at the P2X1 receptor mutants E52C to G96C. The black lines represent the control response, and the gray lines represent the response in the presence of the MTS reagents (1 mM). *B*, the response of mutants E52C to G96C to an EC_{50} concentration of ATP in the presence of MTSES (*i*) and MTSET (*ii*). *, $p < 0.05$; **, $p < 0.01$; ***, $p < 0.001$. Error bars, S.E. Conserved residues are highlighted in black.

use of the smaller positively charged MTSEA (9, 15). At the mutant P2X1 receptors, MTSEA potentiated ATP-evoked responses, and this was associated with an increase in ATP sensitivity ($EC_{50} = 1$ mM compared with control $EC_{50} = 3$ mM for K68C and ~ 3 μ M compared with 10 μ M for K70C; Fig. 6, *C* and *D*). This suggests that it is not just the positive charge but also the size of the side group that is important for determining ATP potency at Lys⁶⁸ and Lys⁷⁰.

The data from the current and previous studies (6, 9) have been mapped onto the homology model for the P2X1 receptor (Fig. 7). This shows that the mutants where MTS reagents had an effect are predominantly located in two clusters (i) around the ATP binding pocket (effects on ATP potency and/or current amplitude) and (ii) on the strands connecting the binding pocket to transmembrane segments (effects on amplitude with no change in potency with the exception of G60C with increased potency). The strands contribute to the vestibule that passes through the center of the receptor (divided into upper, central, and extracellular vestibules). This raised the possibility that the vestibules contribute to the ionic permeation pathway. Cysteine mutants around the apex of the receptor and lining the upper vestibule were unaffected by MTS reagents, suggesting that ions do not flow through the upper vestibule en route to the ionic pore. Several cysteine mutants lining the central vestibule were modified by MTS reagents (Fig. 7). Of particular interest is a ring of three cysteine mutants (G60C, F195C, and K322C)

that are sensitive to MTS reagents that are at the interface of the extracellular and central vestibules. Of these, G60C is at the narrowest part of the constriction between the central and extracellular vestibule (Fig. 7*C*). The positively charged MTSET potentiated currents at this mutant and increased sensitivity to ATP, suggesting that this region may play an important role in transmitting conformational changes in the receptor from the ATP binding site to the channel pore.

DISCUSSION

The x-ray structure of the zebrafish P2X4 receptor has provided a major advance in our understanding of P2X receptors. It has also raised a number of questions regarding the extent of the ATP binding pocket and how agonist binding is translated into channel activation/gating. In this study, cysteine scanning mutagenesis has provided a systematic analysis of the contribution of the region Glu⁵²–Gly⁹⁶ to P2X1 receptor properties. This segment of the receptor can be divided into discrete parts that contribute to ATP binding, partial agonist effects, and channel gating that are flanked by regions corresponding to the bottom and top of the extracellular domain. These findings, as well as previous cysteine-scanning mutagenesis data, have been interpreted with the aid of a homology model of the hP2X1 receptor constructed from the crystal structure of the zebrafish P2X4 receptor. This has given a new insight into agonist binding and channel gating at the P2X1 receptor.

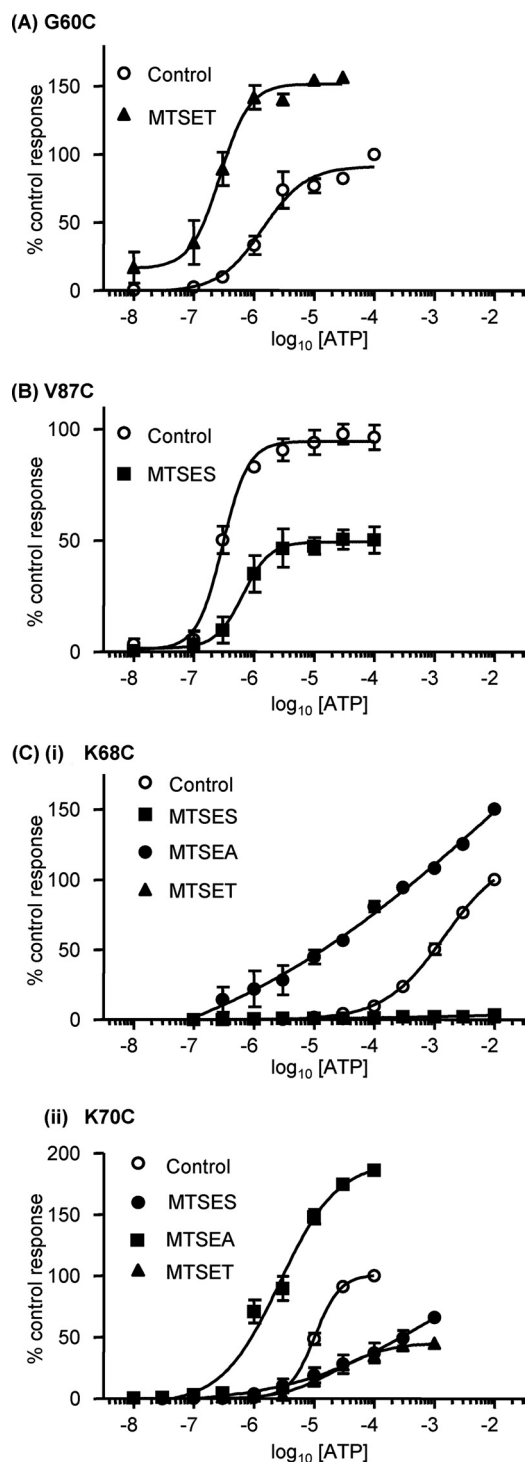


FIGURE 6. Effect of MTS reagents on the ATP potency of P2X1 receptor mutants. A, concentration-response curves of the P2X1 receptor mutant G60C with and without 1 mM MTSET. B, concentration-response curves of the P2X1 receptor mutant V87C with and without 1 mM MTSES. C, concentration-response curves of the P2X1 receptor mutants K68C (i) and K70C (ii) with and without a 1 mM concentration of the charged MTS reagents. All mutants were incubated in the presence of the MTS reagents for 3 h. Error bars, S.E.

In this study, only 3 (K68C, K70C, and F92C) of 45 cysteine mutants had an effect on ATP potency. In total, we have now characterized more than 160 alanine or cysteine mutants (including over 95% of those conserved in mammalian receptors) in the extracellular region of the hP2X1 receptor. Of these,

only mutation at eight residues resulted in a greater than 10-fold decrease in ATP potency, and these form a cluster at the interface between two adjacent P2X receptor subunits (28). We used molecular docking to generate a model of how ATP could bind within this region (Fig. 2). This predicts that the phosphate tail is coordinated by conserved positively charged residues at the receptor surface with the adenine ring buried in the binding pocket. In the present study, K68C and K70C mutants reduced agonist binding, and studies with the MTS reagents demonstrated the importance of positive charge at these residues for ATP action. These results taken together with other mutagenesis studies on P2X1 to -4 receptors (10, 18, 21, 29) support the role of positively charged amino acids Lys⁶⁸, Lys⁷⁰, Arg²⁹², and Lys³⁰⁹ (P2X1 receptor numbering) in coordinating the binding of the negatively charged phosphates of ATP. The model and orientation of the phosphate tail facing outside the pocket are consistent with the activation of P2X receptors with analogues bearing modifications of the phosphate tail (30) and ADP-ribosylation of the P2X7 receptor (31). Two lines of evidence support the binding of the ribose group within the groove formed between adjacent subunits. First, the reduction in ATP potency and agonist binding for the F92C mutant is consistent with the docking simulations of binding the ribose group. Second, the action of BzATP as a partial agonist demonstrates that the binding site can incorporate a benzoyl modification of the ribose ring. It is interesting that mutation of the majority (three of four) of residues (V67C in this study and F100A, F289A, and F289C in Ref. 20) predicted to be involved in binding of the adenine ring had no effect on ATP potency, with the greatest effect of mutation seen at Phe²⁹¹ (P2X1 receptor numbering (20)). However, the effects of mutation at Phe²⁹¹ are dependent on the receptor subtype, with an >40-fold decrease for P2X1; however, only a modest 4-fold decrease was seen at similar mutants at P2X2, -3, and -4 receptors (15, 21). This may be explained by localized differences in the structure or orientation of the Phe residue. This is consistent with differences in the ability to form a disulfide bond between cysteine-substituted Lys⁶⁸ and Phe²⁹¹ receptors (P2X1 receptor numbering) between P2X1 and P2X2 to -4 receptors (32, 33). These results also suggest that no individual residue plays a major role in the binding of the adenine ring, and coordination by several of the residues may be required.

The current study has probed the extent of the binding pocket and demonstrates the importance of the residues that form the back of the ATP binding pocket in regulating receptor properties, as shown by sensitivity to partial agonists, the antagonist suramin, and modification by MTS reagents. The majority (seven of eight) of mutants that showed reduced BzATP efficacy with no change in ATP potency were mapped to the rear/inner cavity of the predicted ATP binding pocket. In addition to these, six of eight residues with a decrease in efficacy to BzATP also showed a reduction in peak response to MTS reagents or a modest increase in suramin sensitivity (supplemental Table i). These results show that mutants not directly predicted to interact with ATP but around the binding pocket can have subtle effects on properties. At the two other families of ligand-gated ion channels (Cys-loop and glutamate), partial agonists have reduced efficacy due to different conformational

Agonist Binding and Gating of P2X1 Receptors

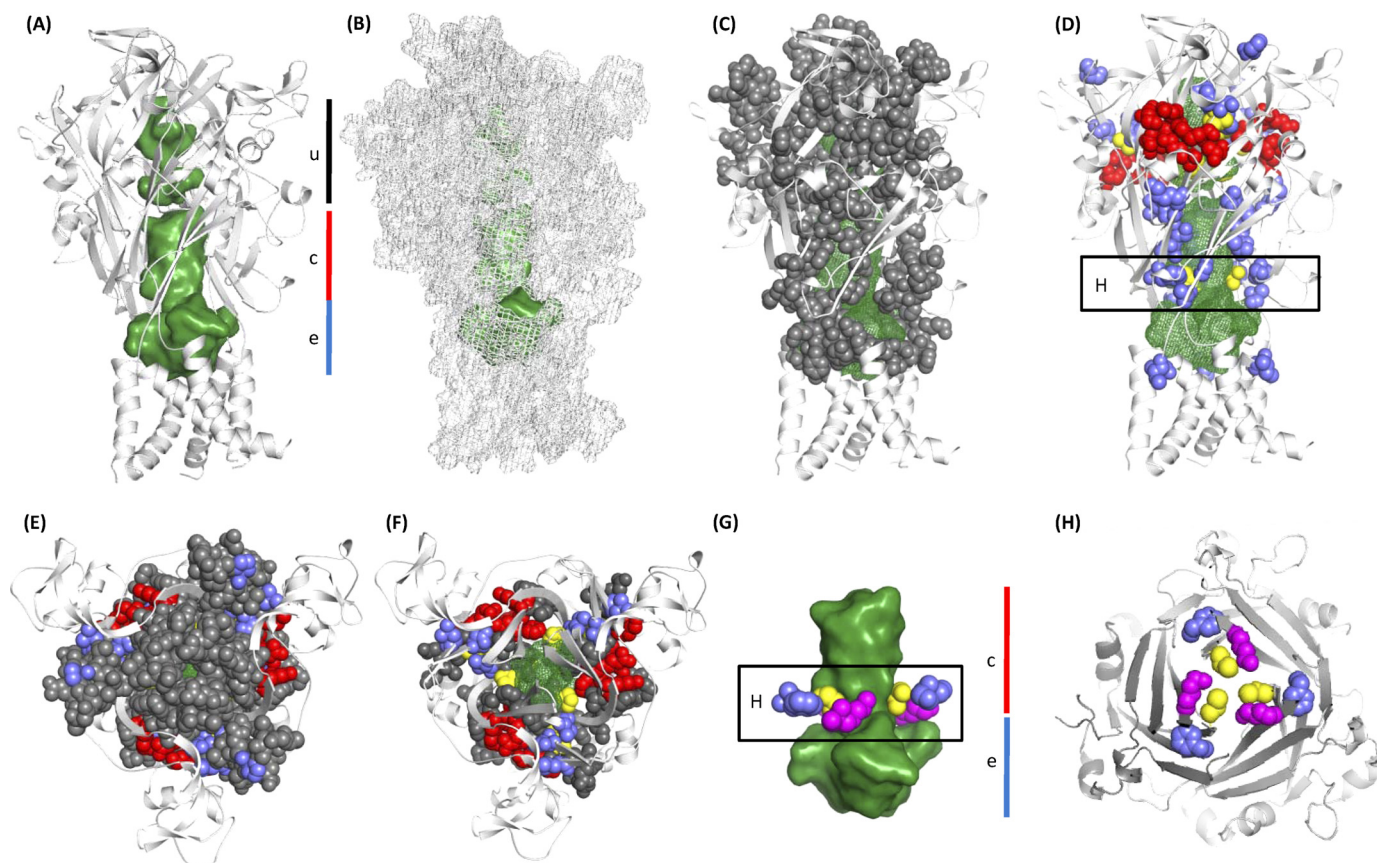


FIGURE 7. Internal vestibules and mapping of MTS reagent data onto the P2X1 receptor homology model. *A* and *B*, overview of the P2X1 model in a schematic representation (*A*) and mesh representation (*B*). The space of the internal vestibules is shown in a green surface representation; black, red, and blue bars indicate the upper vestibule (*u*), central vestibule (*c*), and extracellular vestibule (*e*), respectively. *C* and *D*, mapping the effects of MTS reagents on cysteine mutants onto the P2X1 receptor model. All residues tested are shown as spheres and are colored according to the effect of the MTS reagents. Black, residues where MTS reagents had no effect on current amplitude; blue, residues where the amplitude of responses but not sensitivity to ATP was affected; red, residues where cysteine mutants reduced ATP potency and MTS reagents modified the current amplitude and had a further effect on potency; yellow, residues where cysteine mutation had no effect on ATP potency but MTS reagents modified the amplitude of responses and ATP sensitivity. The vestibules are shown in mesh representation. Residues that were modified by MTS reagents with no effect on ATP potency (blue and yellow) are found predominantly around the central vestibule. *E* and *F*, MTS data from *C* and *D* viewed from the top. In *F*, residues capping the upper vestibule have been removed to better illustrate the residues aligning the upper vestibule. *G*, zoom into the narrow region between the central and extracellular vestibule. MTS-sensitive residues between the two vestibules are shown as spheres for G60C (yellow, cysteine-substituted residue shown), Phe195 (blue), and the adjacent positively charged Lys322 (magenta). *H*, cross-section looking "up" through the receptor from a slice as indicated in the boxes in *D* and *G*. Residues are shown as in *G*.

changes associated with ligand binding before the channel gating step (34, 35). If the same is true at P2X receptors, this further indicates that this region contributes to the agonist binding pocket/conformational changes associated with agonist binding. The increased efficacy of the partial agonists at cysteine-substituted residues Leu⁷² and Ala⁷³ suggests that these mutations facilitate the conformational changes induced in response to partial agonists prior to channel gating.

The proposed ATP binding pocket is ~40 Å distant from the membrane-spanning segments, raising questions of how the binding step is translated into gating of the channel pore. None of the cysteine residues in the connecting region to TM1 had an effect on ATP potency. However, modification by MTS reagents of four of five of the cysteine mutants in the run Gly⁶⁰–Ser⁶⁴ indicates that this region, 10–25 Å from the proposed ATP binding site, contributes to signal transduction/channel properties/regulation of P2X1 receptor currents. These mutants are localized to the central vestibules of the receptor (Fig. 7) (7). Of particular interest is the residue Gly⁶⁰, which lines the base of the central vestibule. Modification of the G60C

mutant with positively charged MTSET produced an ~60% increase in maximal current and an ~6-fold increase in ATP sensitivity. Interestingly, Gly⁶⁰ is adjacent to Lys³²² from another subunit and suggests that modification of G60C with MTSET leads to mutual repulsion between G60C-MTSET and Lys³²². This could lead to a change in channel gating and account for the increase in agonist potency and peak current amplitude. In addition, other residues that form a ring around the interface between the central and extracellular vestibule (F195C, R197C, G321C, and A323C) also were sensitive to modification by MTS reagents (6, 9). These results highlight the importance of the interface between the central and extracellular vestibules in regulating P2X receptor properties. One possibility is that dilation of the ring at the interface between the central and extracellular vestibules transduces ligand binding to the movement of TM2 and opening of the channel pore.

The present study also addresses the likely contributions of the upper and central extracellular vestibules to the ionic permeation pathway. The zebrafish P2X4 receptor structure indicates that the region linking the upper and central vestibules is

too narrow for hydrated ions to pass (7). However, the structure is in a closed state in the absence of ATP, and it is possible that agonist binding leads to a conformational change that could allow ionic permeation from the upper to the central vestibule (7) and then on through the extracellular vestibule to the transmembrane domains and the channel pore. The lack of effects of MTS reagents on ATP evoked responses at cysteine mutants encircling the entrance to and lining the upper vestibule (Fig. 7) demonstrates that the upper vestibule of the receptor does not contribute to the pathway for ionic permeation to the channel pore or provide a conduit for access to the central vestibule. Cysteine mutants in the central vestibule, however, were accessible (shown by MTS reagent sensitivity). Access to the central vestibule seems most likely via the extracellular vestibule. The central vestibule is therefore unlikely to make a major contribution to channeling ions to the pore of the receptor due to its apparent cul-de-sac nature, and this interpretation is consistent with a recent report on P2X2 receptors (36). The extracellular vestibule adjacent to the transmembrane domains is therefore most likely to provide the route of access of ions to the channel pore.

In summary, this study has expanded our understanding of the contribution of the extracellular domain to P2X1 receptor properties. It has provided a model of how agonists bind to the receptor and identified residues lining the base of the central vestibule that contribute to channel gating.

Acknowledgments—We thank Manijeh Maleki-Dizaji for preparation of *Xenopus* oocytes, injections, and some Western blotting and Prof. Martyn Mahaut Smith for comments on the manuscript.

Note Added in Proof—A recent publication (37) also suggests that the adenine ring faces into the ligand binding pocket.

REFERENCES

- North, R. A. (2002) *Physiol. Rev.* **82**, 1013–1067
- Burnstock, G. (2006) *Pharmacol. Rev.* **58**, 58–86
- Khakh, B. S., and North, R. A. (2006) *Nature* **442**, 527–532
- Surprenant, A., and North, R. A. (2009) *Annu. Rev. Physiol.* **71**, 333–359
- Roberts, J. A., Vial, C., Digby, H. R., Agboh, K. C., Wen, H., Atterbury-Thomas, A., and Evans, R. J. (2006) *Pflugers Arch.* **452**, 486–500
- Roberts, J. A., Valente, M., Allsopp, R. C., Watt, D., and Evans, R. J. (2009) *J. Neurochem.* **109**, 1042–1052
- Kawate, T., Michel, J. C., Birdsong, W. T., and Gouaux, E. (2009) *Nature* **460**, 592–598
- Garcia-Guzman, M., Soto, F., Gomez-Hernandez, J. M., Lund, P. E., and Stühmer, W. (1997) *Mol. Pharmacol.* **51**, 109–118
- Roberts, J. A., and Evans, R. J. (2007) *J. Neurosci.* **27**, 4072–4082
- Ennion, S., Hagan, S., and Evans, R. J. (2000) *J. Biol. Chem.* **275**, 29361–29367
- Martí-Renom, M. A., Stuart, A. C., Fiser, A., Sánchez, R., Melo, F., and Sali, A. (2000) *Annu. Rev. Biophys. Biomol. Struct.* **29**, 291–325
- Hooff, R. W., Vriend, G., Sander, C., and Abola, E. E. (1996) *Nature* **381**, 272
- Wiederstein, M., and Sippl, M. J. (2007) *Nucleic Acids Res.* **35**, W407–410
- Verdonk, M. L., Cole, J. C., Hartshorn, M. J., Murray, C. W., and Taylor, R. D. (2003) *Proteins* **52**, 609–623
- Roberts, J. A., Digby, H. R., Kara, M., El Ajouz, S., Sutcliffe, M. J., and Evans, R. J. (2008) *J. Biol. Chem.* **283**, 20126–20136
- Ho, B. K., and Gruswitz, F. (2008) *BMC Struct. Biol.* **8**, 49
- Digby, H. R., Roberts, J. A., Sutcliffe, M. J., and Evans, R. J. (2005) *J. Neurochem.* **95**, 1746–1754
- Jiang, L. H., Rassendren, F., Surprenant, A., and North, R. A. (2000) *J. Biol. Chem.* **275**, 34190–34196
- Jiang, L. H., Rassendren, F., Spelta, V., Surprenant, A., and North, R. A. (2001) *J. Biol. Chem.* **276**, 14902–14908
- Roberts, J. A., and Evans, R. J. (2004) *J. Biol. Chem.* **279**, 9043–9055
- Bodnar, M., Wang, H., Riedel, T., Hintze, S., Kato, E., Fallah, G., Gröger-Arndt, H., Giniatullin, R., Grohmann, M., Hausmann, R., Schmalzing, G., Illes, P., and Rubini, P. (2011) *J. Biol. Chem.* **286**, 2739–2749
- Wolf, C., Rosefort, C., Fallah, G., Kassack, M. U., Hamacher, A., Bodnar, M., Wang, H., Illes, P., Kless, A., Bahrenberg, G., Schmalzing, G., and Hausmann, R. (2011) *Mol. Pharmacol.* **79**, 649–661
- Evans, R. J., Lewis, C., Buell, G., Valera, S., North, R. A., and Surprenant, A. (1995) *Mol. Pharmacol.* **48**, 178–183
- Dunn, P. M., and Blakeley, A. G. (1988) *Br. J. Pharmacol.* **93**, 243–245
- Lambrecht, G., Friebe, T., Grimm, U., Windscheif, U., Bungardt, E., Hildebrandt, C., Bäumert, H. G., Spatz-Kümbel, G., and Mutschler, E. (1992) *Eur. J. Pharmacol.* **217**, 217–219
- Akabas, M. H., Stauffer, D. A., Xu, M., and Karlin, A. (1992) *Science* **258**, 307–310
- Rassendren, F., Buell, G., Newbolt, A., North, R. A., and Surprenant, A. (1997) *EMBO J.* **16**, 3446–3454
- Evans, R. J. (2010) *Br. J. Pharmacol.* **161**, 961–971
- Zemkova, H., Yan, Z., Liang, Z., Jelinkova, I., Tomic, M., and Stojilkovic, S. S. (2007) *J. Neurochem.* **102**, 1139–1150
- Ralevic, V., Hoyle, C. H., and Burnstock, G. (1995) *J. Physiol.* **483**, 703–713
- Adriouch, S., Bannas, P., Schwarz, N., Fliegert, R., Guse, A. H., Seman, M., Haag, F., and Koch-Nolte, F. (2008) *FASEB J.* **22**, 861–869
- Marquez-Klaka, B., Rettinger, J., Bhargava, Y., Eisele, T., and Nicke, A. (2007) *J. Neurosci.* **27**, 1456–1466
- Marquez-Klaka, B., Rettinger, J., and Nicke, A. (2009) *Eur. Biophys. J.* **38**, 329–338
- Jin, R., Banke, T. G., Mayer, M. L., Traynelis, S. F., and Gouaux, E. (2003) *Nat. Neurosci.* **6**, 803–810
- Lape, R., Colquhoun, D., and Sivillotti, L. G. (2008) *Nature* **454**, 722–727
- Kawate, T., Robertson, J. L., Li, M., Silberberg, S. D., and Swartz, K. J. (2011) *J. Gen. Physiol.* **137**, 579–590
- Jiang, R., Lemoine, D., Martz, A., Taly, A., Gonin, S., Prado de Carvalho, L., Specht, A., and Grutter, T. (2011) *Proc. Natl. Acad. Sci. USA* **108**, 9066–9071